Mastozoología Neotropical, 32(1):e01121, Mendoza, 2025
Versión on-line ISSN 1666-0536
https://doi.org/10.31687/saremMN.25.32.01.10.e1121

Copyright © SAREM, 2025
http://www.sarem.org.ar
http://www.sbmz.org

Artículo Original

SHAPE, INTEGRATION, AND MORPHO-FUNCTIONAL TRADE-OFFS IN THE ANTERIOR CRANIUM OF CAVIOIDS IN THE CONTEXT OF CAVIOMORPH RODENTS

Alicia Álvarez[1,2] & Marcos D. Ercoli[1,2]

[1]Laboratorio de Paleontología de Vertebrados, Instituto de Ecorregiones Andinas (INECOA; UNJu-CONICET), San Salvador de Jujuy, provincia de Jujuy, Argentina. [Correspondence: Alicia Álvarez <aalvarez@idgym.unju.edu.ar>]
[2]Instituto de Geología y Minería (UNJu), San Salvador de Jujuy, provincia de Jujuy, Argentina.

ABSTRACT. Cavioidea have a particularly diverging cranio-mandibular anatomy and are ecologically diversified. We analyzed the shape of the anterior cranium and the integration pattern of two modules of this region (rostrum and zygomatic arch-orbital partitions) in 96 caviomorph species to better understand the cavioid morphotype and which functional/ecological factors may explain its configuration. We detected a clear integration pattern between both modules in caviomorphs. Dependence on intense chewing but also on vision to detect predators could lead to the emergence of trade-offs between the orbits and masticatory muscles, and they are interpreted as main factors that could explain covariation patterns of caviomorphs. Cavioids set apart from other caviomorphs regarding the shape of both modules, being an extreme configuration mostly (but not always) characterized by a remarkable long rostrum, a long and dorso-ventrally compressed rostral masseteric fossa, elevated and wide orbits, an anteriorly tilted preorbital bar, and a low zygomatic arch. In caviine cavioids, these traits evolved without following the main integration trend represented in basal cavioids or most other caviomorphs clades. Other caviomorph taxa, such as erethizontids, are also set apart from the main trend. In cavioids, which are cursorial and diurnal rodents with a diet mainly based on grasses and fibrous dietary items, their particular morphological configuration is interpreted as possessing a modified rostral fossa to not affect vision. Caviines do not fit the general covariation trend of modular coupling of caviomorphs and basal cavioids, including representatives with particularly long or short rostrum, in relation to particular ecomorphological trends of each genus.

RESUMEN. FORMA, INTEGRACIÓN Y COMPROMISOS MORFOFUNCIONALES EN EL CRÁNEO ANTERIOR DE LOS CAVIOIDEOS EN EL CONTEXTO DE LOS ROEDORES CAVIOMORFOS. Los cavioideos presentan una anatomía cráneo-mandibular particularmente divergente y son ecológicamente diversos. Aquí analizamos la forma del cráneo anterior y el patrón de integración de dos módulos de esta región (rostro y arco cigomático-órbita) en 96 especies de caviomorfos, para entender mejor el tipo cavioideo y cuáles factores funcionales/ecológicos podrían explicar su configuración. Detectamos un claro patrón de integración entre ambos módulos. La necesidad de una masticación intensa y, a su vez, de una visión adecuada para detectar depredadores podría generar compromisos entre las órbitas y los músculos masticatorios, y estos son interpretados como factores principales al explicar los patrones de covariación en caviomorfos. Los cavioideos se diferencian de otros caviomorfos en cuanto a la forma de ambos módulos, que representan una configuración extrema principalmente (aunque no siempre) caracterizada por un rostro destacablemente largo, una fosa masetérica rostral larga y dorsoventralmente comprimida, órbitas amplias y elevadas, una barra preorbitaria inclinada anteriormente y un arco cigomático bajo. En los cavioideos cavinos, estos rasgos evolucionaron sin seguir la tendencia principal de integración representada en cavioideos basales y muchos

Recibido 01 julio 2024. Aceptado 21 noviembre 2024. Editores asistentes: Dr. David Alfredo Flores y Dra. Amelia Chemisquy

otros clados de caviomorfos. Otros taxones caviomorfos, como los eretizóntidos, también se destacan por diferenciarse de la tendencia principal. En los cavioideos, que son roedores cursoriales y diurnos con una dieta principalmente basada en pastos e ítems dietarios fibrosos, su configuración morfológica particular es interpretada como presentando una fosa rostral modificada para no interferir en la visión. Los cavinos no encajan en la tendencia de covariación general de acople entre módulos observada en otros caviomorfos y cavioideos basales, entre los que se incluyen representantes con rostros largos o cortos, en relación con tendencias ecomorfológicas particulares de cada género.

Key words: Caviidae, geometric morphometrics, masticatory apparatus, zygomasseteric muscles, rostrum.

Palabras clave: Aparato masticatorio, Caviidae, morfometría geométrica, músculos cigomasetéricos, rostro.

Cite as: Álvarez, A. & M. D. Ercoli. 2025. Shape, integration, and morpho-functional trade-offs in the anterior cranium of cavioids in the context of caviomorph rodents. Mastozoología Neotropical, 32(1):e01121. https://doi.org/10.31687/saremMN.25.32.01.10.e1121

INTRODUCTION

Non-protrogomorphous rodents are characterized by the different manners in which specific zygomasseteric bundles reach an advanced position in the cranium and invade the rostrum, increasing the available attachment area or enhancing the mechanical advantage of those muscles for gnawing or chewing functions (Cox & Jeffery 2011; Greaves 2012; Potapova 2020; Becerra & Vassallo 2023, and cites therein). In hystricomorphous rodents, the infraorbital portion of the zygomaticomandibularis muscle is the only advanced zygomasseteric bundle that reaches the rostrum, where it is attached to the rostral masseteric fossa. In relation to this, the infraorbital foramen is expanded for the passage of this advanced bundle and implies the conformation of a laterally extended preorbital bar (vertical ramus of the zygoma; Arnal & Kramarz 2011) between this muscle and the orbit (Hautier et al. 2015; Becerra & Vassallo 2023). Considering the proximity between the orbit, infraorbital foramen, and rostral masseteric fossa, it is expectable the arising of trade-offs between these structures and their functions in hystricomorphous morphotypes, especially in taxa that inhabit open environments, such as cavioids, which highly depend on forward-directed and panoramic vision and powerful grinding to survive (Cox 2008; Sombra 2012; Banks et al. 2015; Hautier et al. 2015; Becerra & Vassallo 2023).

Cavioids are a superfamily of caviomorph rodents that includes small- to large-sized species, such as cavies (e.g., *Microcavia shiptoni*, 185 g), agouties (*Dasyprocta* spp., approx. 4 kg), the Patagonian mara (*Dolichotis patagonum*, 8 kg), and the largest living rodent, the capybara (*Hydrochoerus hydrochaeris*, 70 kg) (Patton et al. 2015; Wilson et al. 2016). Aside from this broad range of body masses, they are diverse in ecological traits, such as diet, which ranges from fruits, stems, and leaves to grasses. Also, they inhabit a wide variety of habitats, from rainforests, wetlands, and open grasslands to dry steppes and rocklands. Related to this, they are also diverse in their locomotory habits and substrate preference; cavies are ambulatory and, in some cases, diggers, maras, agouties, and pacas are cursorials, rocky cavies are rock dwellers, and capybaras display semi-aquatic habits (Campos 1997; Tognelli et al. 1999; Álvarez et al. 2013; Morgan & Álvarez 2013; Patton et al. 2015; Wilson et al. 2016). Several morphological and ecological convergences between cavioids, such as *Dolichotis*, and small ungulates have been proposed; they include the dependence on vision and cursorial abilities to early detect and escape from predators and the preference for open habitats with good sightlines (Campos et al. 2001; Masse & Côté 2009; Sombra 2012; Climaco das Chagas et al. 2019; and cites therein).

In the context of caviomorph rodents, cavioids are divergent with regards to their skull morphology. The cranium is gracile, with a low profile, bearing a long rostrum and diastema, and relatively small to moderate auditory bullae and large orbits. The configuration of the infraorbital foramen and associated structures, such as the preorbital bar is, at first sight, different from that present in other caviomorphs; this foramen is lateromedially and dorsoventrally compressed, and it opens anterolaterally instead anteriorly; also, the preorbital bar is usually anteriorly tilted (anterodorsal-posteroventral directed) (Woods 1972; Álvarez et al. 2023; Becerra & Vassallo 2023), giving a gentle slope change between the rostrum and the zygomatic arch. With regard to the mor-

phology of the mandible, two types can be denoted. The first type is present in dasyproctids and cuniculids and is similar to that of octodontoids, which display relatively short diastema, high coronoid and condylar processes, and marked hystricognathy. The second type would describe that present in caviids (see octodontoid and cavioid types in Vassallo & Verzi 2001). The caviid mandible is shallow and presents a long diastema, low coronoid and condylar processes, low hystricognathy, a posteroventrally projected angular process, and a dorsal masseteric crest connected to the notch for the insertion of the infraorbital part of the zygomaticomandibularis muscle (Vassallo & Verzi 2001; Pérez 2010; Álvarez et al. 2011; Hautier et al. 2011, 2012, 2015; Pérez & Vucetich 2011; Álvarez & Pérez 2019; Spataru & Spataru 2023). Caviids also present euhypsodont molars, with lobular shape in occlusal view, that are specialized for grinding tough elements (Álvarez & Pérez 2019; Boivin et al. 2022), such as grasses, which are a main component of their diet, especially in caviines (e.g., Campos 1997; Tognelli et al. 1999; Wilson et al. 2016). This divergent morphology is particularly exacerbated in caviines, which also deviates from general trends established for caviomorphs and other cavioids. Indeed, the mandibular shape of caviines departs from the covariation and allometric common trends that explain mandible shape changes among caviomorph rodents, specifically because of the elongation of the jaw and the high reduction of the size of the coronoid process differing from other small caviomorphs (Álvarez et al. 2020). Typical caviomorph covariation patterns among skull components, i.e., between cranial modules and mandible, or between different mandibular modules (e.g., alveolar and muscular sectors) are not followed by caviines, resulting in an extremely modified mandibular shape (Álvarez et al. 2015, 2020).

Among cavioids, and related to the marked differences in mandibular morphology, two muscular configurations were described. Dasyproctids and cuniculids present a myological structure similar to that present in other caviomorphs (Woods 1972; Álvarez & Pérez 2019). On the other hand, caviids stand out because of their derived configuration of the masticatory musculature, which is associated with their particular craniomandibular anatomy (Pérez 2010; Pérez & Vucetich 2011; Álvarez & Pérez 2019). Main, outstanding features are the large development and marked horizontal disposition achieved by the masseter superficialis, masseter profundus, and pterygoideus medialis muscles (Woods 1972; Cox & Jeffery 2011; Álvarez et al. 2023; Spataru & Spataru 2023). On the other hand, particularly for caviines, the infraorbital part of the zygomaticomandibularis muscle is relatively reduced, as well as the zygomatic arch part of this muscle. This is related to the fact that the origin and insertion areas are very close because the zygomatic arch is displaced ventrally and the insertion notch for the infraorbital part and the dorsal masseteric crest are dorsally positioned. All these traits contribute, together with the horizontalized main pterygomasseter bundles, to exert more efficient grinding movements (Vassallo & Verzi 2001; Pérez & Vucetich 2011; Álvarez & Pérez 2019; Álvarez et al. 2023).

Until now, very few studies have analyzed the covariation of cranial modules in caviomorphs or cavioids (Álvarez et al. 2015; Perdue 2017; Álvarez & Flores 2019). The first study assessed the covariation between three cranial modules (base, vault, and face) and the mandible; the main result was the detection of tight covariation among cranial modules and that this may be driven by allometry and ecology (Álvarez et al. 2015). Perdue (2017) proposed schemes of cranial modules for caviomorph rodents different from what is expected in previous proposals (Goswami 2006; Goswami & Polly 2010; Álvarez et al. 2015). Álvarez & Flores (2019) explored different cranial modular schemes for caviids and found that the most probable model of modularity was that represented by six modules (anterior oral-nasal; molar; orbit; zygomatic-pterygoid; vault; basicranium; Goswami 2006; Goswami & Polly 2010). These authors found that the oral-nasal and orbit modules were the most correlated (integrated) modules and that the oral-nasal and molar modules are the best-defined modules, followed by the zygomatic-pterygoid one (Álvarez & Flores 2019: table 4).

Considering previous observations that showed a particular reconfiguration of these muscles and their bony attachments in cavioids (Vassallo & Verzi 2001; Hautier et al. 2011; Álvarez et al. 2020, 2023; see also Becerra & Vassallo 2023), analyzing the patterns of covariation could be revealing because it would allow us to better understand cavioid morphologies, how their osteo- and myological peculiarities are related to each other, and which main functional and evolutionary factors are related to each morphotype. So, in this contribution, we studied cranial shape variation and its modular structure in cavioids in comparison with other caviomorph rodents, and we got into the group to analyze the differences between the different morphotypes detected within this superfamily. Particularly, we focused on the anterior cranium, which contains the structures from

which zygomasseteric muscles originate, such as the rostral masseteric fossa and the zygomatic arch, and the orbit and preorbital bar, which covary with zygomasseteric osteomyological structure (Cox 2008; Hautier et al. 2011). We aimed to get deep in the comprehension of the osteomyological configuration and the evolution of this peculiar rodent group that is strongly divergent from other caviomorphs, revisiting and analyzing in a comprehensive way all the recent advances made about this caviomorph group.

MATERIALS AND METHODS

The analyzed sample of caviomorphs included crania of 272 specimens representing 96 species (Appendix 1; Supplementary Material Appendix S1).

The shape of the anterior region of the cranium was represented by two-dimensional coordinates of 16 landmarks and 20 semilandmarks (**Fig**. 1), which were digitized on photographs of the lateral view of the cranium using TpsDig 2.18 (Rohlf 2015). Following previous studies on cranial shape variation of caviomorphs (see Álvarez & Arnal 2015; Olivares et al. 2020), landmarks and semilandmarks were defined as follows. Landmarks: 1, most posterior point of the alveolar margin of the incisors; 2, most dorsal point of the alveolar margin of the incisors; 3, anterior upper end of premaxillary bone (on the sagittal plane); 4, anterior end of the nasal bone; 5, meeting between lacrimal and frontal bones on the antero-dorsal margin of orbit; 6, most dorsal point of the jugal-maxilla suture; 7, dorsal meeting between jugal and squamosal bones; 8, postero-dorsal end of cranial glenoid fossa; 9, most posterior point of the jugal-squamosal suture; 10, most ventral point of the jugal-maxilla suture; 11, most anterior point of the zygomatic arch; 12, the junction between the maxillar-premaxillar suture and ventral margin of rostrum; 13, antero-ventral end of rostral masseteric fossa; 14, postero-ventral point of the lateral margin of infraorbital foramen; 15, postorbital process; 16, most antero-dorsal point in the anterior margin of the preorbital bar. Semilandmarks: 17-19, between landmarks 10 and 11; 20-21, between landmarks 9 and 10; 22-23, between landmarks 1 and 12; 24-26, between landmarks 13 and 16; 27-28, between landmarks 14 and 16; 29-31, between landmarks 5 and 15; 32-33, between landmarks 5 and 6; 34-36, between landmarks 6 and 7. In our sample, all cavioid genera were included except for *Cuniculus* because of its particular cranial morphology that precluded the correct positioning of some landmarks and semilandmarks.

The raw-coordinate dataset was subjected to a generalized Procrustes analysis (GPA; Rohlf & Slice 1990) to remove differences related to scaling, translation, and rotation. During this procedure, semilandmarks were slid using the minimum bending energy criterion (Mitteroecker & Gunz 2009). The centroid size (CS) of each configuration was considered as a proxy of the size of the anterior cranium for each specimen. The mean values of the aligned coordinates and CS were used in further analyses. These values are presented in Supplementary Material Appendix S2.

A Principal Component (PC) analysis was carried out to explore shape variation among caviomorph rodents and the position of cavioids in the cranial shape morphospace (i.e., ploting of the first three PCs). The broken-stick method was used to select informative components. Because of the wide range of sizes among caviomorphs, allometry was estimated through a regression between aligned coordinates and log-transformed CS (logCS).

For the analysis of integration and modularity between cranial modules, two partitions (modules) were considered: rostrum (RoM) and zygomatic arch and orbit (ZyOM). The rostrum, as defined here, is linked to the origin of the infraorbital part of the zygomaticomandibularis muscle. The zygomatic arch is the origin of the remaining part of that muscle (the arch portion of the zygomaticomandibularis muscle) and the origin of the masseter bundles (e.g., Woods 1972; Álvarez et al. 2023). The selection of these two modules was based on the consideration that the two regions serve as the origin for different muscular bundles and that the presence of the former is what defines a hystricomorphous morphotype, in turn presenting remarkable known variations in caviomorphs (see Introduction section). Landmarks 1-4, 12-14, 16 and semilandmarks 22-28 were assigned to RoM; landmarks 5-11, 15 and semilandmarks 17-21, 29-36 were assigned to ZyOM (**Fig**. 1). A first approach was to consider both modules conjointly, splitting the aligned coordinates into the two module configurations after the common GPA (on the cranial shape data). Alternatively, the raw coordinates of each module were separated before running two separate GPA for each dataset. This approach allows performing the integration analysis but does not allow testing modularity because modules are treated separately. The results of both approaches may differ because the former analysis works on datasets that preserve the information related to orientation, scaling, and position between modules, and this information is lost in the second approach (Klingenberg 2009; Baab 2013). Integration, i.e., the degree in which morphological traits covary (Adams & Collyer 2016), was evaluated using a PLS (partial least squares) analysis that describes the maximal covariation between two sets of variables (in the present study, the shape of two cranial modules) and the statistic *r*-PLS which is the output of this analysis (Mitteroecker & Bookstein 2007; Adams 2016). Modularity, i.e., when correlations among traits are concentrated in specific regions (modules) of a structure but are weaker than those of other regions (Adams 2016), was assessed through the CR (covariance ratio) value, which describes covariation between modules relative to the covariation within modules (Adams 2016). These analyses were run with and without taking phylogenetic structure into account. The statistical significance of both statistics was evaluated using permutation tests with 9,999 iterations. Finally, the perpendicular distances of each species and selected caviomorph clades to the main covariation line along the first pair of PLS were computed as a measure of the decoupling from the general integration (covariation between modules) trend.

All procedures and analyses were carried out using standard functions (phylo.integration and phylo.modularity in the case of the phylogenetic comparative analyses) available in the *geomorph* R package (version 4.0.6, Adams & Otarola-Castillo 2013; Baken et al. 2021; Adams et al. 2024) and R environment (version 4.3.3.; R Core Team 2024). In the case of the phylogenetic comparative analyses, phylo.integration and phylo.modularity functions were

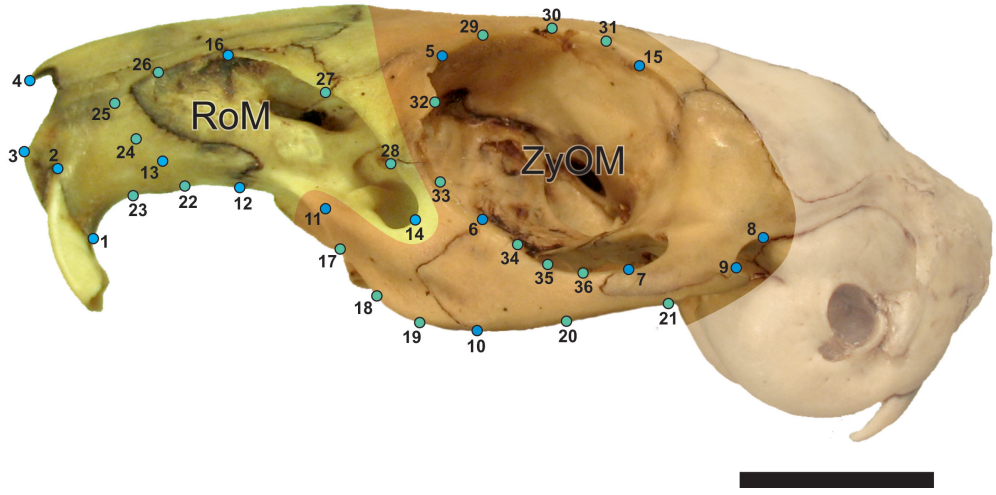

Fig. 1. Landmark design used in this study, exemplified on *Galea spixii* (FMNH 20283). Blue points, landmarks; aquamarine points, semilandmarks. RoM: rostrum module (yellow background); ZyOM: zygomatic arch and orbit module (orange background). See the Materials and Methods section for landmark definitions and assignments to modules. Scale bar = 1 cm.

used. The broken-stick method was implemented in PAST software (Hammer et al. 2001).

RESULTS

For the anterior cranial shape analysis, six axes were retained as informative by the broken-stick method. The first three components of the PCA explained 63.22% of the total shape variation (PC1 = 33.43%; PC2 = 15.48%; PC3 = 14.32%) (**Fig**. 2), while the next three components explained only 17.4% of the remaining variation (PC4 = 7.96%; PC5 = 5.71%; PC6 = 3.73%).

Most caviomorph families separated from each other in the morphospace built up by the first two PCs. Erethizontids and dasyproctids, hydrocherines, and dolichotines represented the extremes of the distribution, both on negative and positive values of the PC1, respectively. Chinchillids, ctenomyids, abrocomids, some octodontids, and a few echimyids were segregated towards negative values of the PC2. Most echimyids and octodontids showed an overlapped distribution near the center of the morphospace. Major shape changes toward negative values of PC1 were related to crania with short rostra and shortened rostral masseteric fossae and the maxillary-premaxillary suture close to the anterior end of the zygomatic arch, small orbits with high ventral border, and dorso-ventrally expanded zygomatic arches (**Fig**. 3). This shape corresponded to that displayed by erethizontids (**Fig**. 2). On the other hand, towards positive values of PC1, main changes were linked to longer rostra with expanded rostral masseteric fossae, larger orbits with the ventral border below the level of the ventral aspect of the diastema, and thinner zygomatic arches with the jugal bone anteroposteriorly short. This shape corresponded to that displayed by most cavioids (**Fig**. 2). Dolichotines are similar-shaped to those taxa but they present relatively wider zygomatic arches in their anterior portion, and the most anteriorly extended point of the rostrum was that of the premaxillary bone, while in dasyproctids the nasals were the most anteriorly extended. Shape changes towards negative values of the PC2 were related to larger rostra with anteriorly expanded rostral masseteric fossae and an anteroposteriorly stretched ventral portion of the anterior part of the diastema, smaller orbits, and taller zygomatic arches with the jugal bone occupying a large portion of the preorbital bar whose most antero-dorsal margin is dorsally located (**Fig**. 3). This shape corresponded to that of some ctenomyids, like *Ctenomys torquatus*, and the chinchillid *Lagidium* which approached extreme negative values of the PC2. Those echimyids that were located on negative values of PC2 (*Clyomys*, *Euryzygomatomys*, and capromyines) were characterized by shorter rostra and rostral masseteric fossae, smaller orbits, and taller zygomatic arches. Similar scores were presented by the octodontid *Spalacopus* and *Aconaemys*. Shape changes towards positive values of the PC2 were linked to longer rostra due to the anterior ex-

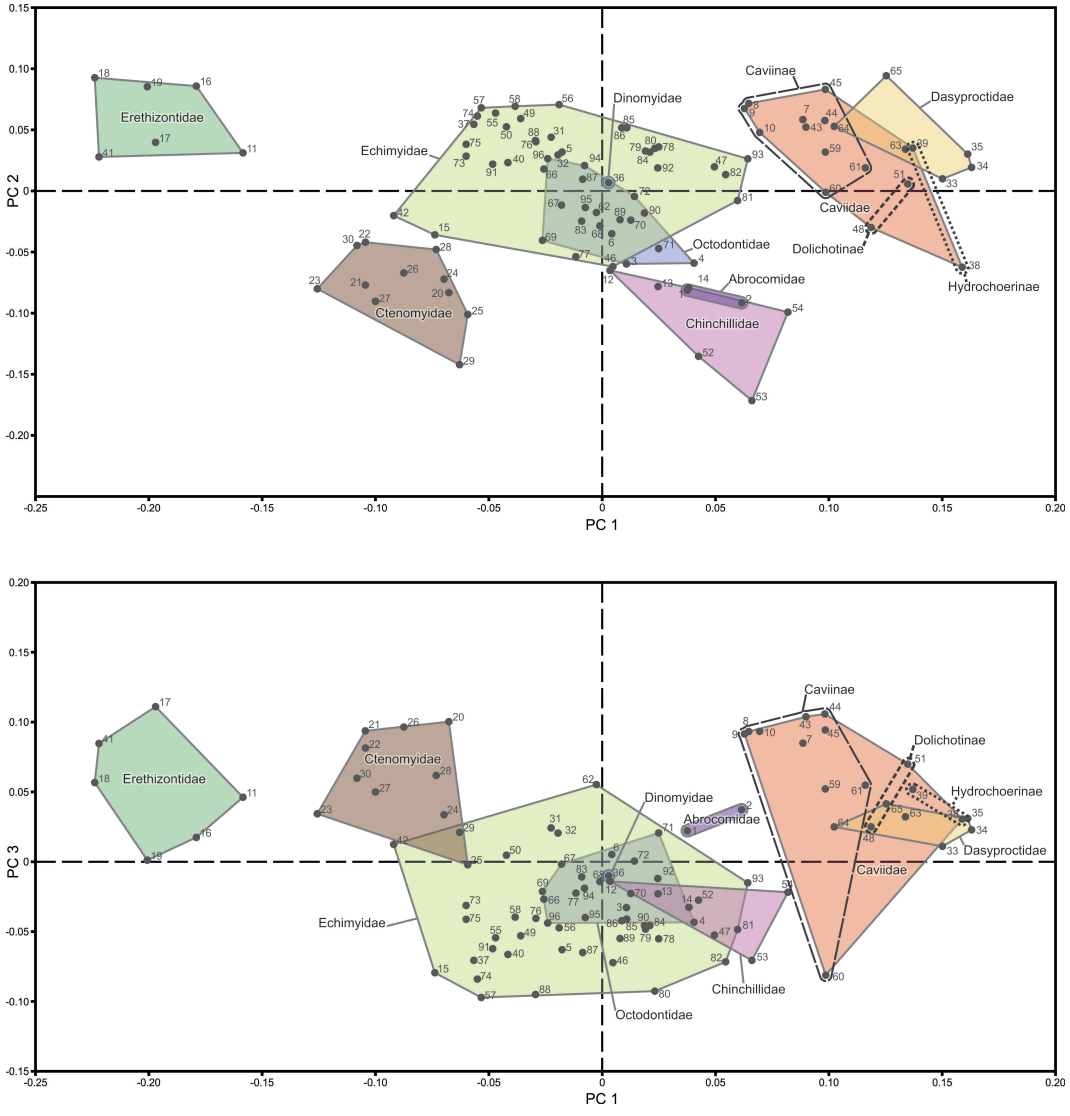

Fig. 2. First three axes of the principal component analysis of anterior cranium shape: upper box: PC1 vs. PC2, lower box: PC1 vs. PC3. Polygons indicate the distribution of representatives of different caviomorph families and caviid subfamilies: violet, Abrocomidae; dark orange, Caviidae; lilac, Chinchillidae; brown, Ctenomyidae; light orange, Dasyproctidae; light blue, Dinomyidae; light green, Echimyidae; dark green, Erethizontidae; blue, Octodontidae; long dashed line, Caviinae; short dashed line, Dolichotinae; dotted line, Hydrochoerinae. See deformation grids illustrating variation at the extremes of PCs in **Figure** 3. See Appendix 1 for correspondence between numbers and studied species.

pansion of the premaxillary and nasal bones, shorter diastemata, wider orbits, and thinner zygomatic arches. Taxa presenting shapes more similar to this description are echimyids. Caviines were located on positive and central values of the PC2, with *Microcavia* showing the lowest values (**Fig**. 2). They present long rostra with large rostral masseteric fossae, wide orbits, and tall zygomatic arches at the level of the preorbital bar, which is markedly anteriorly (from dorso-anterior to ventro-posterior) tilted. With regards to the latter feature, *M. niata* differs markedly from the other species of the genus given that it presents a preorbital bar that is vertically oriented. *Cavia* and *Galea* differ from *Microcavia* in some traits, such as the shape of the upper margin of the zygomatic arch. On the other hand, hydro-

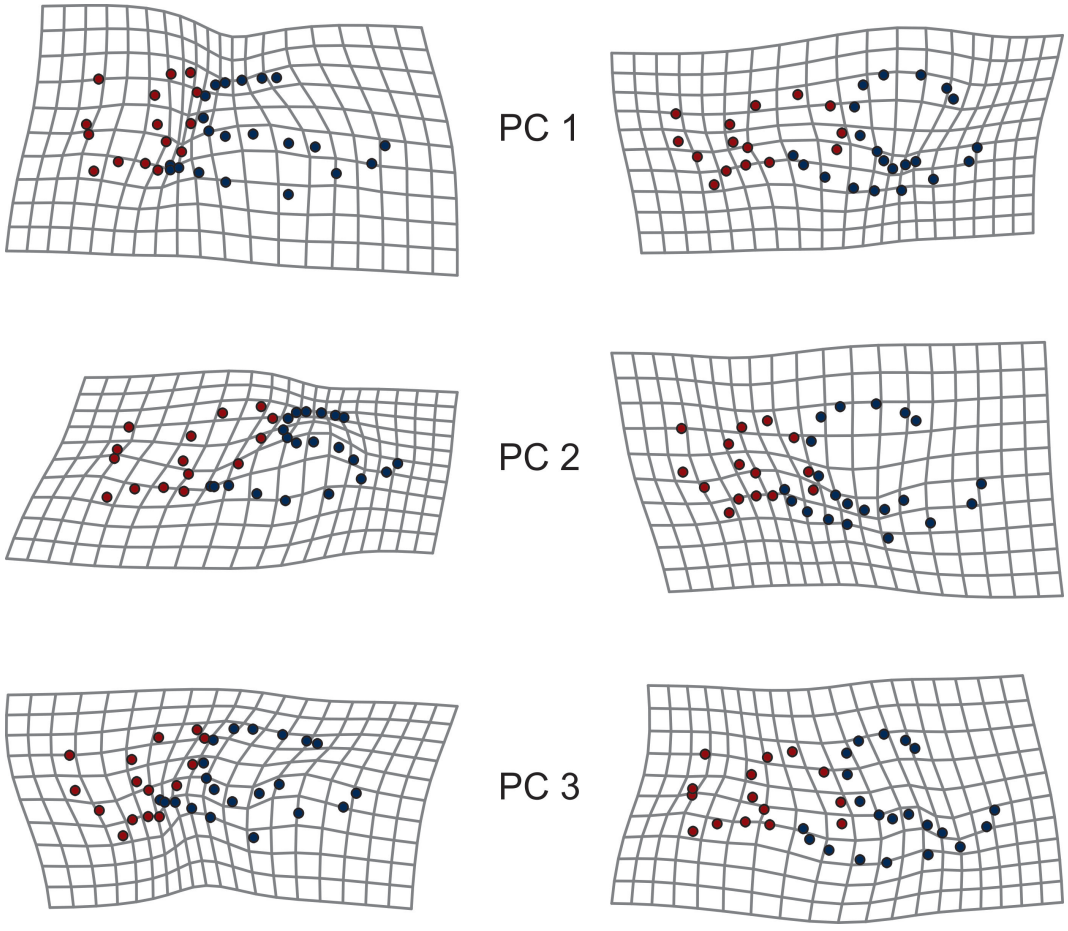

Fig. 3. Deformation grids of the extremes of the first three principal components illustrated in **Figure** 2. Left grid, negative extreme; right grid, positive extreme. Red dots, RoM; blue dots, ZyOM (See Materials and Methods sections for abbreviations of modules).

choerines and *Dolichotis* presented very long rostra with expanded rostral masseteric fossa, orbits that are dorsally located and present their upper margins projecting dorsally with respect to the cranial roof, and a tall zygomatic arch with a vertically oriented preorbital bar.

Along the PC3, some erethizontids, some ctenomyids, abrocomids (separated from chinchillids), *Cavia*, and *Galea* separated towards the most extreme positive values while the majority of the echimyids and octodontids, chinchillids, and *Microcavia niata* (which separates significantly from the other caviines) were located towards central and negative values. This pattern is in relation to a shortening of the diastema and the proximity of the anterior root of the zygomatic arch and the anteroventral limit of the rostral masseteric fossa in the latter taxa (**Figs**. 2, 3).

Along the PC4, dinomyids, most erethizontids, chinchillids, and *M. niata* separated toward negative values; this, in relation to a taller posterior portion of the zygomatic arch and smaller orbit in comparison to other taxa. Several echimyids and ctenomyids were located towards positive values of PC4 in relation to opposite shapes. PC5 and PC6 did not show a clear pattern of taxa ordination towards positive values but did segregate specific taxa on negative values, such as *M. niata* (PC5) and *Capromys* and *Hydrochoerus* (PC6) (morphospaces not shown).

Allometry was largely not significant, as logCS explained only 7% (p-value = 0.33). Octodontids and almost all echimyids have the smallest logCS values

with relatively similar shape around configurations associated with short rostra and rostral masseteric fossa, relatively small orbits, and tall zygomatic arches. Erethizontids have similar shapes to those taxa but are larger. Although weak, the trend towards larger logCS values relates to crania with longer rostra and rostral masseteric fossa, wider orbits, and relatively thinner zygomatic arches. Taxa with large logCS values are *Hydrochoerus*, dolichotines, dasyproctids, and *Lagostomus*. Caviines present similar shapes but have small logCS values.

Integration analysis between modules rostrum (RoM) and zygomatic arch plus orbit (ZyOM) when aligned simultaneously showed that both cranial modules are highly integrated (r-PLS = 0.912, *p*-value = 0.0001), but the variation within each module was greater than the covariation between modules resulting in relatively, although weakly, independent modules (CR = 0.936, CI = 0.894-0.980, *p*-value = 0.012). The results when phylogeny was taken into account were similar (r-PLS = 0.877, *p*-value = 0.0001; CR = 0.850, CI = 0.802-0.933, *p*-value = 0.0005). The shape changes of the ZyOM module towards negative values of PLS1 were related to an antero-posterior shortening of the anterior part of the zygomatic arch together with a dorso-ventral extension of this structure and a shrinking of the orbit; they covaried with changes in RoM associated with a shortening of the rostral masseteric fossa. An opposite trend can be described for positive values of PLS1 (**Figs**. 4 and 5). The distribution of taxa along this first dimension of covariation (PLS1 ZyOM, PLS1 RoM; **Fig**. 4) was as follows: erethizontids located on extreme negative values; octodontids, most echimyids, and ctenomyids showed negative values, having the latter the most negative values together with the echimyid *Clyomys* and *Euryzygomatomys*; some echimyids, *Dinomys*, abrocomids, chinchilloids, and cavioids showed positive values; among them, dolichotines, hydrochoerines, and particularly dasyproctids displayed the most extreme positive values. Erethizontids and caviids (particularly caviines) showed a large dispersion with respect to the main trend of covariation (mean distances: Erethizontidae = 0.059, Caviidae = 0.057, Caviinae = 0.060). Among caviines, *Microcavia* showed lower values of PLS1 RoM and higher values of PLS1 ZyOM, while the contrary occurred for *Galea* and most species of *Cavia* (*C. porcellus* located near the main covariation line; see **Fig**. 4). Other taxa deviated from the main trend, such as abrocomids (mean distances: 0.088), *Lagostomus* (distance: 0.083), and some echimyids, such as *Mesomys*, *Olallamys* (mean distance: 0.081). Compared to these values, the other caviomorphs showed a low dispersion with respect to the general trend (e.g., mean distances: Octodontidae = 0.022, Echimyidae = 0.028, Ctenomyidae = 0.025, Chinchillinae = 0.033, Dasyproctidae = 0.010) (see **Fig**. 4).

The integration analysis of both modules considered as separate datasets (with independent GPA) gave a similar result; RoM and ZyOM were largely integrated (r-PLS = 0.814, *p*-value = 0.0001). Along the PLS1, the distribution of taxa was similar, although ctenomyids, abrocomids, and chinchillids obtained more negative values on both first dimensions (see **Fig**. 5). As described for the analysis in which both modules were simultaneously aligned when landmark partitions were aligned separately, erethizontids and caviids (particularly caviines) showed again a remarkably large dispersion with respect to the main trend of covariation.

DISCUSSION

Cavioids, and particularly caviids, have been recognized as a markedly derived rodent group with particular ecomorphological adaptations, acquired along an evolutionary history linked to the exploitation of open environments, and with most of their extant representatives with grass-eating, epigean, diurnal, and cursorial habits (Gambaryan 1974; Vassallo & Verzi 2001; Rocha-Barbosa et al. 2002; Hautier et al. 2012, 2015; Sombra 2012; Álvarez & Pérez 2019; Climaco das Chagas et al. 2019; Vassallo & Rocha-Barbosa 2020; see Introduction section). In this study, we confirmed and quantified how cavioids differentiate from other caviomorph rodents in the cranial morphology and the shape of each of both modules here considered (see **Figs**. 2, 4). Indeed, each main caviomorph clade (e.g., family) presents particular and relatively circumscribed, anterior cranial shape diversity (see **Fig**. 2) intimately related to the long-standing evolutionary history of caviomorphs (e.g., Álvarez et al. 2013). In general, cavioids are the caviomorphs with the longest rostra, elevated orbits, and dorso-ventrally compressed and antero-posteriorly extended rostral masseteric fossae (Woods 1972; Vassallo & Verzi 2001; Hautier et al. 2015; Álvarez et al. 2023). A long rostrum, as that present in cavioids, can be related to a marked decoupling of chewing and gnawing functions and large available space for muscles dedicated to food processing and accommodation (e.g., buccinator) (Turnbull 1970; Álvarez et al. 2023). The low-positioned zygomatic arch of cavioids can be related to the horizontalization of the muscular fibers of the masseter superficialis and profundus in relation to

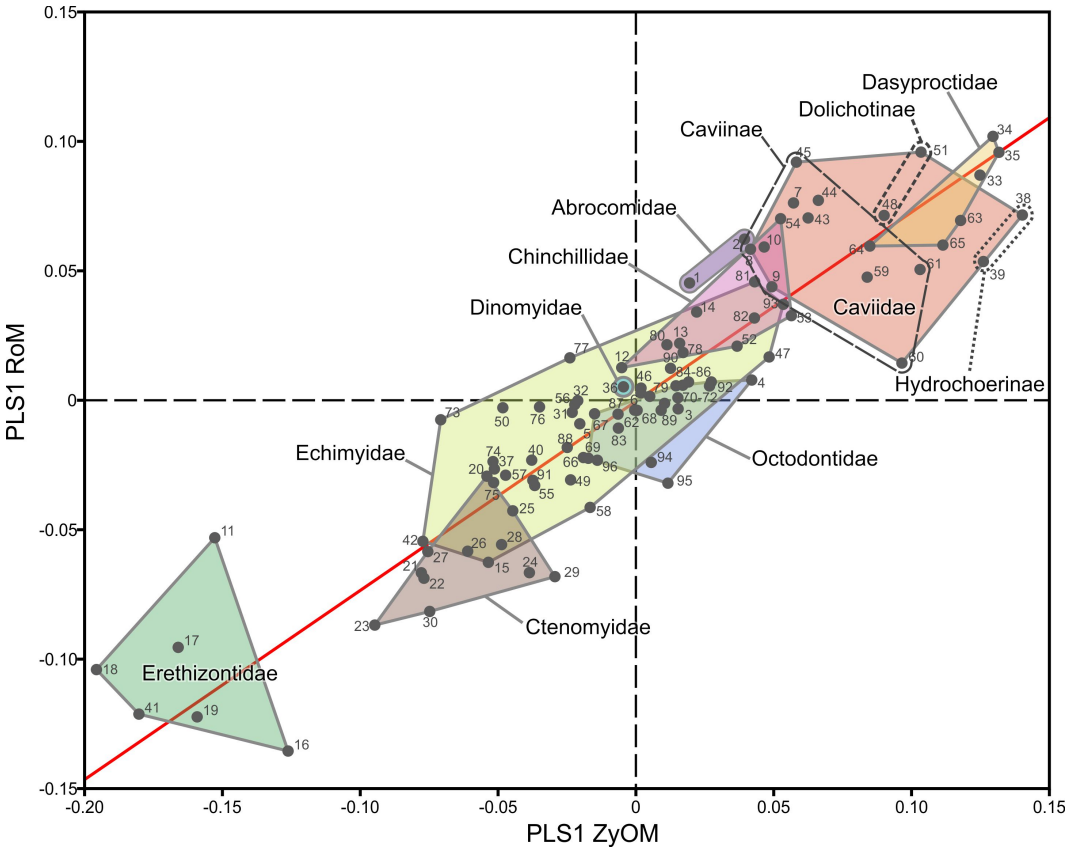

Fig. 4. Covariation patterns along the first dimensions (PLS1) of a partial least square analysis of the aligned Procrustes coordinates of the RoM and ZyOM modules using simultaneous Procrustes fit. Polygons indicate the distribution of representatives of different caviomorph families and caviid subfamilies: violet, Abrocomidae; dark orange, Caviidae; lilac, Chinchillidae; brown, Ctenomyidae; light orange, Dasyproctidae; light blue, Dinomyidae; light green, Echimyidae; dark green, Erethizontidae; blue, Octodontidae; long dashed line, Caviinae; short dashed line, Dolichotinae; dotted line, Hydrochoerinae. See deformation grids illustrating variation at the extremes of PLS1 in **Figure** 5. See Appendix 1 for correspondence between numbers and studied species.

enhanced grinding movements (Álvarez et al. 2023). Indeed, the low condyle position and the posteriorly extended angular process were interpreted in the same way for caviid cavioids and other grinding rodent clades (Vassallo & Verzi 2001; Hautier et al. 2015; Álvarez et al. 2020; Potapova 2020). In cavioids, the elongation of the rostrum is given mainly by the antero-posterior expansion of the maxillary bone and the rostral masseteric fossa. Additionally, there is a reconfiguration of the transition zone between the two analyzed modules (ZyOM, RoM), reflected in an expansion of the dorsal extreme of the preorbital bar (lacrimal and frontal bones; see Cox 2008). In his study, Cox (2008) recognized two morphological extremes for the rostral configuration of hystricomorphous rodents. One of these corresponds to caviomorphs with rostral masseteric fossa anteriorly extended, exemplified by *Lagostomus*, *Hydrochoerus*, and *Dasyprocta*. According to Cox (2008), in these taxa and resembling ungulate artiodactyl morphotypes, there is a large contribution of the lacrimal bone to the conformation of the posterior part of the rostrum, which is expanded, greatly in agreement with our results. In our study, these changes are associated with the increasing size and dorsal location of the orbit and a particularly modified zygomatic arch that locates ventrally, although the degree of association is different among cavioids.

As also suggested for other hystricomorphous morphotypes, the spatial interaction between masticatory apparatus and orbits would affect each other and, eventually, imply the rise of trade-offs between

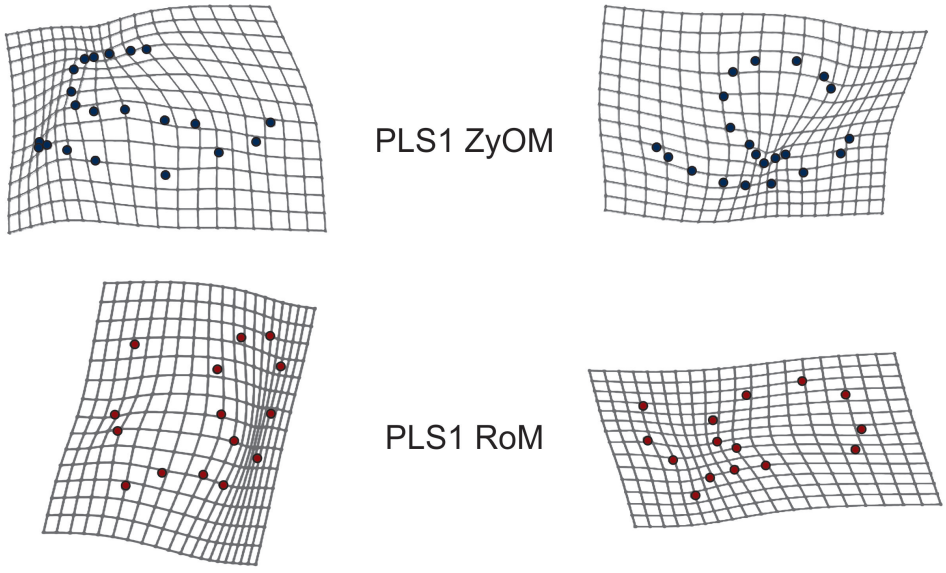

Fig. 5. Deformation grids of the first dimensions (PLS1) of a partial least square analysis of the aligned Procrustes coordinates of the RoM and ZyOM modules (see **Figure** 4). Left grid, negative extreme; right grid, positive extreme. Red dots, RoM; blue dots, ZyOM (See the Materials and Methods section for abbreviations of modules).

their morphologies and functions (Cox 2008; Hautier et al. 2015). In line with this, Hautier et al. (2012) proposed that the location of the temporalis and zygomasseteric bundles far away from the orbit is also an adaptation to reduce potential interferences between mastication movements that could distort the lateral orbital margin and the visual acuity. The latter characteristic would be a priority in cavioids that are potential prey during daytime (Cox 2008, see Heesy 2004, 2008). Following this, the shape and location of the infraorbital foramen and the widening of the dorsal margin of the preorbital bar could contribute to the distancing between the eye and related structures and masticatory muscles. Moreover, the hystricomorphous condition would imply the potential obstruction of the anterior sector of the visual field. This may compromise the performance of those taxa that require panoramic vision to detect predators and particularly forward-directed vision to see the terrain during escape running (Banks et al. 2015). This inference would imply that the modifications of the rostrum and masticatory apparatus configuration are subordinated to a lesser interference in the visual field. Interestingly, in some small artiodactyl ungulates, the relative position of the orbits (Cox 2008; Banks et al. 2015) and of the masseteric bundles that invade the rostrum are reminiscent of that of cavioids; however, in those ungulates, the origin of these muscles from a rostral masseteric crest that does not markedly protrude laterally from the rostrum (e.g., Turnbull 1970; Allouch 2018) does not imply an obstacle for a clear vision, contrary to the hystricomorphy. The ventral displacement of the rostral masseteric fossa and the infraorbital foramen would contribute to increasing the visual field in cavioids. The changes in the relative position of the orbit and rostral masseteric fossa can explain the tilting of the preorbital bar observed in most of the cavioids.

Alternatively, Becerra & Vassallo (2023) recently proposed that the configuration of the preorbital bar could be linked to changes to the masticatory biomechanics. In this regard, the anterior tilting of the preorbital bar would be directly related to the resultant line of action of the zygomasseteric complex. This relation seems to be supported by our data on cavioids. In turn, the combination of large and elevated orbits and a rostral masseteric fossa with a low profile would also be a relevant factor to consider for the development of an anterodorsal-posteroventral directed preorbital bar in cavioids. Therefore, the existence of more than one relevant factor is expected to explain the variation of a structure linked to others that vary according to such different demands.

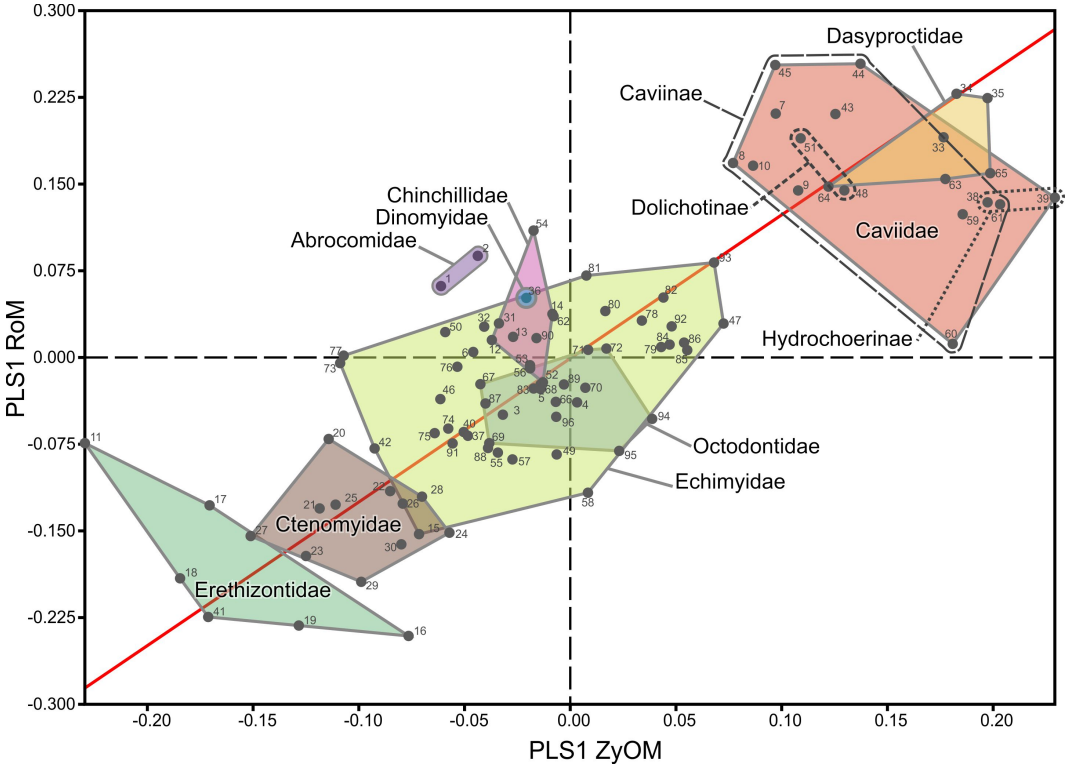

Fig. 6. Covariation patterns along the first dimensions (PLS1) of a partial least square analysis of the aligned Procrustes coordinates of the RoM and ZyOM modules using separate Procrustes fit. Polygons indicate the distribution of representatives of different caviomorph families and caviid subfamilies: violet, Abrocomidae; dark orange, Caviidae; lilac, Chinchillidae; brown, Ctenomyidae; light orange, Dasyproctidae; light blue, Dinomyidae; light green, Echimyidae; dark green, Erethizontidae; blue, Octodontidae; long dashed line, Caviinae; short dashed line, Dolichotinae; dotted line, Hydrochoerinae. See deformation grids illustrating variation at the extremes of PLS1 in **Figure** 5. See Appendix 1 for correspondence between numbers and studied species.

Added to these features, among cavioids, caviines, and to a lesser degree other caviids, display some myological traits that make them stand out. For example, caviines have a very little-developed infraorbital portion of the zygomaticomandibularis muscle (4-9% of the total masticatory muscle mass). These values represent half or less of what was recorded for other cavioids, such as *Dasyprocta* (17%, own data not previously published) and caviomorphs in general, for which data are available (e.g., Becerra et al. 2014; Álvarez et al. 2023; Ercoli et al. 2023; **Fig**. 7). This change in muscular proportions is related to more lateromedially flattened rostra and infraorbital foramina (Woods 1972; Álvarez et al. 2023; see **Fig**. 7). The relative reduction of the infraorbital portion of the zygomaticomandibularis muscle is linked to the greater importance of other zygomasseteric bundles (mm. masseter superficialis and profundus), which in turn are horizontalized. This is related to the lower importance in the efforts of the incisive bite compared of the effort of grinding in the dietary type of caviines, which is linked to a grass-eating specialization (Vassallo & Verzi 2001; Hautier et al. 2015; Álvarez et al. 2020, 2023). Also, it has been highlighted for caviids that the insertions of the portions of the zygomaticomandibularis muscle are markedly dorsal on the lateral surface of the mandible, and the angular process is largely posteriorly extended (see **Fig**. 7). These features are in relation to a marked division of tasks, that is, a vertical line of action for a powerful chewing pressure vs. a more horizontal line of action for propalinal movements during cropping and chewing (e.g., Maynard Smith & Savage 1956; Álvarez & Pérez 2019; Álvarez et al. 2023). The set of all osteomyological modifications of the configuration of the masticatory apparatus of caviines differentiates them not only from the rest of the caviomorphs but also from the morphotype already

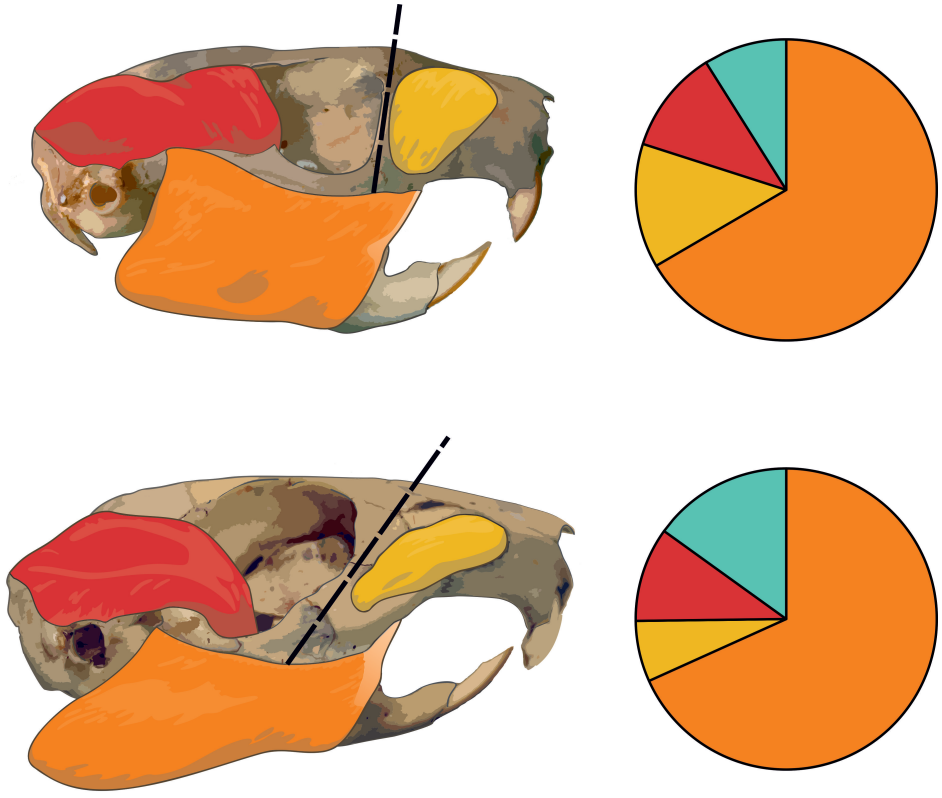

Fig. 7. Schematic representation of osteomuscular configurations of a non-cavioid caviomorph (exemplified by *Kannabateomys*, see Álvarez & Arnal 2015) and a caviine (exemplified by *Galea*, see Álvarez et al. 2023). Pie charts represent typical myological proportions of non-cavioid and caviine caviomorphs, computed as mean values from different species compiled by Álvarez et al. (2023). Yellow, infraorbital portion of the zygomaticomandibularis muscle; orange, other portions of the zygomasseteric complex; red, temporalis muscle; pale blue, pterygoid complex; dashed line, main axis of the preorbital bar.

derived from other cavioids, with the tendency to enhance grinding even more.

In addition to having particular osteomyological traits, caviines do not fit the general covariation model of caviomorphs between the ZyOM and RoM modules that make up the anterior cranium (according to the present study), as their covariation is decoupled or, at least, is not coupled in the same way as it is in other caviomorphs. When the covariation pattern of the alveolar and muscular modules of the mandible was previously analyzed (Álvarez et al. 2020), a similar distribution pattern was observed, in which caviids, with *Cavia*'s species as the extreme, were separated from the general trend of the rest of the caviomorphs by presenting the angular process more markedly elongated posteriorly and very low condylar and coronoid processes (Vassallo & Verzi 2001; Álvarez et al. 2020).

Particularly for *Microcavia* species, conformable to their position in the covariation morphospace, they display shortened rostra compared to what would be expected according to the pattern detected for caviomorphs with *M. niata* as the most extreme case in this sense (indeed, *niata* is the phonetics for "*ñata*" that in Spanish means literally "not protruding rostrum"; from the original description of the species: "Skull very peculiarly shortened…"; Thomas 1898: p.282). This species also stands out because of the more dorsally located zygomatic arch and a vertical preorbital bar. So, *Microcavia* reverts to a more "generalized" configuration of the rostrum reminiscent of many other non-cavioid caviomorphs (the position of *Microcavia*, particularly *M. niata*, on PLS1 RoM can be compared with that of other caviomorphs; see **Fig**. 4). On the other hand, the shape of the module ZyOM (i.e., low zygomatic arch and elevated orbit)

is similar to that of other cavioids. The reversions of rostral features are added to other already recognized in literature, as those described for teeth morphology ("demolarized" deciduous fourth premolar; more oblique direction of chewing; Álvarez & Pérez 2019; Boivin et al. 2022 and cites therein). Worth mentioning is that these changes could be associated with reversions in ecological aspects, which include being the least grass-eater, the most fossorial, the most climber, and the smallest of all caviids, and in some of these aspects, than the remaining cavioids in general (e.g., Tognelli et al. 1999; Wilson et al. 2016).

Distinctly, although caviines of the genera *Cavia* and *Galea* also display a decoupling of the cranial modules compared to the main covariation trend of caviomorphs, they do it in the opposite direction (see **Fig**. 4). In them, the rostrum is longer, the rostral masseteric fossa is extended antero-posteriorly, the preorbital bar is tilted, and the zygomatic arch is low; features similar to other cavioids (see the beginning of the Discussion section). The elongation of the rostrum does not seem to be driven by the shape changes in the ZyOM nor by the need for greater space for the development of the infraorbital portion of the zygomaticomandibularis muscle, which is reduced in these species, but by other ecomorphological issues, such as selection and processing of food and avoiding interference in the visual field, as already mentioned for cavioids in general. Particularly long faces are also present in non-cavioid caviomorphs such as abrocomids and some chinchillids (*Lagostomus*, *Chinchilla* spp.; see **Fig**. 4; see also Results section), which also move away from the main integration trend of caviomorphs, probably in relation to the fact that these species also present grass-eating habits (see Álvarez et al. 2020). In relation to the ZyOM module, although the zygomatic arch of *Cavia* and *Galea* has a derived cavioid morphology, the presence of an orbit not as large or elevated as those of other cavioids indicates an intermediate morphology between non-cavioid and cavioid caviomorphs, differing from the markedly derived configuration of the rostrum and mandible (Vassallo & Verzi 2001; Álvarez et al. 2020, 2023). Finally, the reason behind the relaxed, or modified, coupling between the modules of the anterior cranium in caviines could be linked to a lesser relevance of the rostrum as part of the origin of the zygomasseteric complex in comparison to the zygomatic arch, as evidenced by its morphology and the muscular proportions, differing in this way from other hystricomorphous rodents.

Although they are not the focus of this work, it is worth mentioning that erethizontids are a group of caviomorphs particularly different in their cranial morphology, to such a degree that in the constructed morphospaces they do not have areas of overlap with any other group of caviomorphs. They stand out because the analyzed modules are not markedly integrated in the way that occurs in other caviomorphs, and they present morphologies opposite to the cavioids, with short rostra, antero-posteriorly compressed rostral masseteric fossae, verticalized preorbital bars, and very robust and elevated zygomatic arches. In line with this, previous studies have commented on differences in the masticatory myology of *Erethizon* (the only erethizontid with data of masticatory muscular masses) (Allen 1880; Turnbull 1970; Samuels 2009; Álvarez et al. 2023), including much more developed temporal and pterygoid muscles than those of other caviomorphs, and there are also great differences in ecological-dietary aspects for some of its representatives, such as *Erethizon*, which presents lignivorous habits (e.g., Samuels 2009), suggesting the need that they should be analyzed as a particular morphotype.

CONCLUSIONS

The shape of the anterior cranium of caviomorph rodents reflects the wide ecological and myological diversity of these rodents traceable along their long-standing evolutionary history. There is a general trend for caviomorphs in which the rostral and zygomatic arch-orbital regions strongly covary, and this tendency is maintained in most clades, including basal cavioids. In this study, cavioids were characterized as a markedly derived rodent group in their rostral and orbital morphology, in addition to other already recognized eco-morphological features. The main integration trend of caviomorphs is here interpreted as linked to potential trade-offs between demands on vision and masticatory functions. Furthermore, a wide, panoramic vision and a specialized masticatory apparatus should hit it off in a cavioid configuration. Specifically, caviines represent a particularly derived morphotype and do not fit the general covariation model of caviomorphs and basal cavioids, differentiating from the main tendency of coupling between anterior cranial modules and including representatives with particularly long or short rostrum, in relation to particular ecomorphological trends of each genus. Other caviomorph clades, such as erethizontids, also depart from the main shape and integration trends and should be the focus of further studies.

ACKNOWLEDGMENTS

The authors thank S. Bogan (CFA), R. Barquez, M. Díaz (CML), R. Ojeda (IADIZA), P. Teta, G. Cassini, S. Lucero (MACN), I. Olivares, D. Verzi (MLP), D. Romero, N. Martino (MMP), M. de Vivo (MZUSP), and B. Patterson (FMNH) for granting access to specimens under their care. We are grateful to two anonymous reviewers for their valuable comments that greatly improved the manuscript. Thanks to N. Cortés-Delgado and J. S. Salgado-Ahumada for photographs of some specimens. Thanks to M. Collyer and D. C. Adams for helping us with some methodological issues. Funding information. PICT-2018-01237, PICT-2021-I-INVI-00406, PICT-2020-SERIEA-02985, Agencia I+D+i (Agencia Nacional de Promoción de la Investigación, el Desarrollo Tecnológico y la Innovación). PIP 11220210100278CO, CONICET (Consejo Nacional de Investigaciones Científicas y Técnicas). N949, UNLP (Universidad Nacional de La Plata).

LITERATURE CITED

Adams, D. C. 2016. Evaluating modularity in morphometric data: challenges with the RV coefficient and a new test measure. Methods in Ecology and Evolution 7:565-572. https://doi.org/10.1111/2041-210X.12511

Adams, D. C., & M. L. Collyer. 2016. On the comparison of the strength of morphological integration across morphometric datasets. Evolution 70:2623-2631. https://doi.org/10.1111/evo.13045

Adams, D. C., & E. Otarola-Castillo. 2013. Geomorph: an R package for the collection and analysis of geometric morphometric shape data. Methods in Ecology and Evolution 4:393-399. https://doi.org/10.1111/2041-210X.12035

Adams, D., M. Collyer, A. Kaliontzopoulou, & E. Baken. 2024. Geomorph: Software for geometric morphometric analyses. R package version 4.0.8. https://cran.r-project.org/package=geomorph

Allen, H. 1880. On the temporal and masseter muscles of mammals. Proceedings of the Academy of Natural Sciences of Philadelphia 32:385-396.

Allouch, M. G. 2018. A comparative study of the physical characteristics of the masticatory muscles in sheep. International Journal of Animal Science 2:1023.

Álvarez, A., & M. Arnal. 2015. First approach to the paleobiology of extinct *Prospaniomys* (Rodentia, Hystricognathi, Octodontoidea) through head muscle reconstruction and the study of craniomandibular shape variation. Journal of Mammalian Evolution 22:519-533. https://doi.org/10.1007/s10914-015-9291-z

Álvarez, A., & D. A. Flores. 2019. Skull morphology in herbivorous mammals: macropodids (Metatheria, Diprotodontia, Macropodidae) and caviids (Eutheria, Rodentia, Hystricomorpha) as a comparative study case. Mastozoología Neotropical 26:241-254. https://doi.org/10.31687/saremMN.18.26.2.0.02

Álvarez, A., & M. E. Pérez. 2019. Deep changes in masticatory patterns and masseteric musculature configurations accompanied the eco-morphological evolution of cavioid rodents (Hystricognathi, Caviomorpha). Mammalian Biology 96:53-60. https://doi.org/10.1016/j.mambio.2019.03.009

Álvarez, A., S. I. Pérez, & D. H. Verzi. 2011. Ecological and phylogenetic influences on mandible shape variation of South American caviomorph rodents (Rodentia: Hystricomorpha). Biological Journal of the Linnean Society 102:828-837. https://doi.org/10.1111/j.1095-8312.2011.01622.x

Álvarez, A., S. I. Pérez, & D. H. Verzi. 2013. Ecological and phylogenetic dimensions of the cranial shape diversification in South American caviomorph rodents (Rodentia: Hystricomorpha). Biological Journal of the Linnean Society 110:898-913. https://doi.org/10.1111/bij.12164

Álvarez, A., S. I. Pérez, & D. H. Verzi. 2015. The role of evolutionary integration in the morphological evolution of the skull of caviomorph rodents (Rodentia: Hystricomorpha). Evolutionary Biology 42:312-327. https://doi.org/10.1007/s11692-015-9326-7

Álvarez, A., M. D. Ercoli, & D. H. Verzi. 2020. Integration and diversity of the caviomorph mandible (Rodentia: Hystricomorpha): assessing the evolutionary history through fossils and ancestral shape reconstructions. Zoological Journal of the Linnean Society 188:276-301. https://doi.org/10.1093/zoolinnean/zlz071

Álvarez, A., M. D. Ercoli, M. Boivin, A. M. Ortiz Tejerina, & S. R. Moyano. 2023. Head myology of wild cavies (Caviidae, Caviomorpha) and functional implications of hystricomorphous and hystricognathous configurations. Journal of Mammalian Evolution 30:747-771. https://doi.org/10.1007/s10914-023-09656-6

Arnal, M., & A. G. Kramarz. 2011. First complete skull of an octodontoid (Rodentia, Caviomorpha) from the Early Miocene of South America and its bearing in the early evolution of Octodontoidea. Geobios 44:435-444. https://doi.org/10.1016/j.geobios.2010.12.003

Baab, K. L. 2013. The impact of superimposition choice in geometric morphometric approaches to morphological integration. Journal of Human Evolution 65:689-692. https://doi.org/10.1016/j.jhevol.2013.07.004

Baken, E., M. Collyer, A. Kaliontzopoulou, & D. Adams. 2021. Geomorph v4.0 and gmShiny: enhanced analytics and a new graphical interface for a comprehensive morphometric experience. Methods in Ecology and Evolution 12:2355-2363. https://doi.org/10.1111/2041-210X.13723

Banks, M. S., W. W. Sprague, J. Schmoll, J. A. Q. Parnell, & G. D. Love. 2015. Why do animal eyes have pupils of different shapes? Science Advances 1:e1500391. https://doi.org/10.1126/sciadv.1500391

Becerra, F., A. I. Echeverría, A. Casinos, & A. I. Vassallo. 2014. Another one bites the dust: bite force and ecology in three caviomorph rodents (Rodentia, Hystricognathi). Journal of Experimental Zoology. Part A, Ecological Genetics and Physiology 321:220–232. https://doi.org/10.1002/jez.1853

Becerra, F., & A. I. Vassallo. 2023. Shape analysis of the preorbital bar in caviomorph rodents. Journal of Morphology 284:e21646. https://doi.org/10.1002/jmor.21646

Boivin, M., A. Álvarez, & M. D. Ercoli. 2022. Integration patterns of cheek teeth and ecomorphological evolution in grinding herbivores: the case of caviine rodents (Caviomorpha: Caviidae). Zoological Journal of the Linnean Society 196:1094-1116. https://doi.org/10.1093/zoolinnean/zlac005

Campos, C. M. 1997. Utilización de recursos alimentarios por mamíferos medianos y pequeños del desierto del monte. Ph.D. Thesis, Universidad Nacional de Córdoba, Córdoba, Argentina.

Campos, C. M., M. F. Tognelli, & R. A. Ojeda. 2001. *Dolichotis patagonum*. Mammalian Species 652:1-5. https://doi.org/10.2307/0.652.1

Climaco das Chagas, K. S., A. I. Vassallo, F. Becerra, A. Echeverría, M. Fiuza de Castro Loguercio, & O. Rocha-Barbosa. 2019. Locomoción en el roedor más veloz, la mara *Dolichotis patagonum* (Caviomorpha; Caviidae; Dolichotinae). Mastozoología Neotropical 26:65-79. https://doi.org/10.31687/saremMN.19.26.1.0.06

Cox, P. G. 2008. A quantitative analysis of the Eutherian orbit: correlations with masticatory apparatus. Biological Reviews 83:35-69. https://doi.org/10.1111/j.1469-185X.2007.00031.x

Cox, P. G., & N. Jeffery. 2011. Reviewing the morphology of the jaw-closing musculature in squirrels, rats and guinea pigs with

contrast enhanced microCT. Anatomical Record 294:915-928. https://doi.org/10.1002/ar.21381

Ercoli, M. D., A. Álvarez, N. M. Warburton, C. M. Janis, E. G. Potapova, S. W. Herring, G. H. Cassini, J. Tarquini, & A. Kuznetsov. 2023. Myology of the masticatory apparatus of herbivorous mammals and a novel classification for a better understanding of herbivore diversity. Zoological Journal of the Linnean Society 198:1106-1155. https://doi.org/10.1093/zoolinnean/zlac102

Gambaryan, P. P. 1974. How Mammals Run. Wiley, New York, USA.

Goswami, A. 2006. Cranial modularity shifts during mammalian evolution. American Naturalist 168:270-280. https://doi.org/10.1086/505758

Goswami, A., & P. D. Polly. 2010. The influence of modularity on cranial morphological disparity in Carnivora and Primates (Mammalia). PLoS ONE 5:e9517. https://doi.org/10.1371/journal.pone.0009517

Greaves, W. S. 2012. The mammalian jaw: a mechanical analysis. Cambridge University Press, Cambridge, UK.

Hammer, Ø., D. A. T. Harper, & P. D. Ryan. 2001. PAST: paleontological statistics software package for education and data analysis. Palaeontologia Electronica 4:4. Available from https://www.nhm.uio.no/english/research/resources/past/

Hautier, L., R. Lebrun, S. Saksiri, J. Michaux, M. Vianey-Liaud, & L. Marivaux. 2011. Hystricognathy vs sciurognathy in the rodent jaw: a new morphometric assessment of hystricognathy applied to the living fossil *Laonastes* (Diatomyidae). PLoS ONE 6:e18698. https://doi.org/10.1371/journal.pone.0018698

Hautier, L., R. Lebrun, & P. G. Cox. 2012. Patterns of covariation in the masticatory apparatus of hystricognathous rodents: implications for evolution and diversification. Journal of Morphology 273:1319-1337. https://doi.org/10.1002/jmor.20061

Hautier, L., P. G. Cox, & R. Lebrun. 2015. Grades and clades among rodents: the promise of geometric morphometrics. Evolution of the rodents: advances in phylogeny, functional morphology, and development (P. G. Cox, & L. Hautier, eds.). Cambridge University Press, Cambridge, UK.

Heesy, C. P. 2004. On the relationship between orbit orientation and binocular visual field overlap in mammals. Anatomical Record 281A:1104-1110.

Heesy, C. P. 2008. Ecomorphology of orbit orientation and the adaptive significance of binocular vision in primates and other mammals. Brain, Behavior & Evolution 71:54-67. https://doi.org/10.1159/000108621

Klingenberg, C. P. 2009. Morphometric integration and modularity in configurations of landmarks: tools for evaluating a priori hypotheses. Evolution & Development 11:405-421.

Masse, A., & S. D. Côté. 2009. Habitat selection of a large herbivore at high density and without predation: trade-off between forage and cover? Journal of Mammalogy 90:961-970. https://doi.org/10.1644/08-MAMM-A-148.1

Maynard Smith, J., & R. J. G. Savage. 1956. The mechanics of mammalian jaws. School Science Review 141:289-301.

Mitteroecker, P., & F. Bookstein. 2007. The conceptual and statistical relationship between modularity and morphological integration. Systematics Biology 56:818-836. https://doi.org/10.1080/10635150701648029

Mitteroecker, P., & P. Gunz. 2009. Advances in geometric morphometrics. Evolutionary Biology 36:235-247. https://doi.org/10.1007/s11692-009-9055-x

Morgan, C. C., & A. Álvarez. 2013. The humerus of South American caviomorph rodents: shape, function and size in a phylogenetic context. Journal of Zoology 290:107-116. https://doi.org/10.1111/jzo.12017

Olivares, A. I., A. Álvarez, D. H. Verzi, S. I. Pérez, & N. A. de Santi. 2020. Unravelling the distinctive craniomandibular morphology of the Plio-Pleistocene *Eumysops* in the evolutionary setting of South American octodontoid rodents (Hystricomorpha). Palaeontology 63:443-458. https://doi.org/10.1111/pala.12464

Patton, J. L., U. F. J. Pardiñas, & E. D'Elía. 2015. Mammals of South America. Vol. 2. Rodents. University of Chicago Press, Chicago, USA.

Perdue, G. V. 2017. The evolution of cranial modularity and integration in the Caviomorpha lineage (Mammalia, Rodentia). Ms. Thesis, University of Oregon, Eugene, USA.

Pérez, M. E. 2010. A new rodent (Cavioidea, Hystricognathi) from the middle Miocene of Patagonia, mandibular homologies, and the origin of the crown group Cavioidea sensu stricto. Journal of Vertebrate Paleontology 30:1848-1859. https://doi.org/10.1080/02724634.2010.522432

Pérez, M. E., & M. G. Vucetich. 2011. A new extinct genus of Cavioidea (Rodentia, Hystricognathi) from the Miocene of Patagonia (Argentina) and the evolution of cavioid mandibular morphology. Journal of Mammalian Evolution 18:163-183. https://doi.org/10.1007/s10914-011-9154-1

Potapova, E. G. 2020. Morphofunctional transformations of the jaw muscles in rodent evolution. Biology Bulletin Reviews 10:394-406. https://doi.org/10.1134/S2079086420050072

R Core Team. 2024. R: a language and environment for statistical computing. Foundation for Statistical Computing, Vienna. Available at: http://www.R-project.org

Rocha-Barbosa, O., D. Youlatos, J. P. Gasc, & S. Renous. 2002. The clavicular region of some cursors Cavioidea (Rodentia: Mammalia). Mammalia 66:413-421. https://doi.org/10.1515/mamm.2002.66.3.413

Rohlf, F. J. 2015. Tpsdig, version 2.15; tpsrelw, version 1.54. University of New York at Stony Brook, New York, USA. Available at: https://www.sbmorphometrics.org/

Rohlf, F. J., & D. Slice. 1990. Extensions of the Procrustes method for the optimal superimposition of landmarks. Systematic Zoology 39:40-59. https://doi.org/10.2307/2992207

Samuels, J. X. 2009. Cranial morphology and dietary habits of rodents. Zoological Journal of the Linnean Society 156:864-888. https://doi.org/10.1111/j.1096-3642.2009.00502.x

Sombra, M. S. 2012. Foraging, predation and sociality in maras (*Dolichotis patagonum*). Ms. Thesis, University of Illinois at Chicago, Chicago, USA.

Spataru, C., & M. C. Spataru. 2023. Peculiarities of the masticatory apparatus of guinea pigs (*Cavia porcellus*). Journal of Applied Life Sciences and Environment 56:127-138. https://doi.org/10.46909/alse-561090

Tognelli, M. F., C. E. Borghi, & C. M. Campos. 1999. Effect of gnawing by *Microcavia australis* (Rodentia, Caviidae) on *Geoffroea decorticans* (Leguminosae) plants. Journal of Arid Environments 41:79-85. https://doi.org/10.1006/jare.1998.0470

Thomas, O. 1898. On some new mammals from the neighbourhood of Mount Sahama, Bolivia. The Annals and Magazine of Natural History 277-283.

Turnbull, W. D. 1970. Mammalian masticatory apparatus. Fieldiana (Geol) 18:147-356.

Vassallo, A. I., & O. Rocha-Barbosa. 2020. Limb bone stress in the mara *Dolichotis patagonum* (Caviomorpha; Caviidae; Dolichotinae). Hystrix, Italian Journal of Mammalogy 1:35-39. https://doi.org/10.4404/hystrix\T1\textendash00297-2020

Vassallo, A. I., & D. H. Verzi. 2001. Patrones craneanos y modalidades de masticación en roedores caviomorfos (Rodentia, Caviomorpha). Boletín de la Sociedad de Biología de Concepción, Chile 72:145-151.

Wilson, D. E., T. E. Lacher Jr., & R. A. Mittermeier. 2016. Handbook of mammals of the world. Vol 6. Lagomorphs and Rodents I. Lynx Edicions, Barcelona, Spain.

Woods, C. A. 1972. Comparative myology of jaw, hyoid and pectoral appendicular regions of New and Old World hystricomorph rodents. Bulletin of the American Museum of Natural History 147:115-198.

Appendix 1: List of analyzed taxa, indicating the number of specimens (N) included. # indicates the numbers used in the figures. Ca, Cavioidea; Ch, Chinchilloidea; E, Erethizontoidea; O, Octodontoidea.

#	Species	Family	N	#	Species	Family	N
1	*Abrocoma bennettii*	Abrocomidae (O)	3	49	*Isothrix bistriata*	Echimyidae (O)	3
2	*A. cinerea*	Abrocomidae (O)	4	50	*Kannabateomys amblyonyx*	Echimyidae (O)	4
3	*Aconaemys porteri*	Octodontidae (O)	4	51	*Kerodon rupestris*	Caviidae (Ca)	5
4	*A. sagei*	Octodontidae (O)	1	52	*Lagidium viscacia*	Chinchillidae (Ch)	6
5	*Callistomys pictus*	Echimyidae (O)	1	53	*L. wolffsohni*	Chinchillidae (Ch)	1
6	*Capromys pilorides*	Echimyidae (O)	3	54	*Lagostomus maximus*	Chinchillidae (Ch)	5
7	*Cavia aperea*	Caviidae (Ca)	6	55	*Lonchothrix emiliae*	Echimyidae (O)	2
8	*C. fulgida*	Caviidae (Ca)	3	56	*Makalata armata*	Echimyidae (O)	3
9	*C. porcellus*	Caviidae (Ca)	4	57	*M. didelphoides*	Echimyidae (O)	3
10	*C. tschudii*	Caviidae (Ca)	4	58	*Mesomys hispidus*	Echimyidae (O)	2
11	*Chaetomys subspinosus*	Erethizontidae (E)	2	59	*Microcavia australis*	Caviidae (Ca)	8
12	*Chinchilla chinchilla*	Chinchillidae (Ch)	3	60	*M. niata*	Caviidae (Ca)	2
13	*C. intermedia*	Chinchillidae (Ch)	1	61	*M. shiptoni*	Caviidae (Ca)	3
14	*C. lanigera*	Chinchillidae (Ch)	5	62	*Myocastor coypus*	Echimyidae (O)	2
15	*Clyomys laticeps*	Echimyidae (O)	2	63	*Myoprocta acouchy*	Dasyproctidae (Ca)	2
16	*Coendou bicolor*	Erethizontidae (E)	2	64	*M. milleri*	Dasyproctidae (Ca)	1
17	*C. rotschildi*	Erethizontidae (E)	2	65	*M. pratti*	Dasyproctidae (Ca)	3
18	*C. rufescens*	Erethizontidae (E)	3	66	*Mysateles prehensilis*	Echimyidae (O)	2
19	*C. spinosus*	Erethizontidae (E)	3	67	*Octodon bridgesi*	Octodontidae (O)	1
20	*Ctenomys australis*	Ctenomyidae (O)	4	68	*O. degus*	Octodontidae (O)	4
21	*C. bicolor*	Ctenomyidae (O)	2	69	*O. lunatus*	Octodontidae (O)	2
22	*C. bonettoi*	Ctenomyidae (O)	2	70	*O. ricardojeda*	Octodontidae (O)	2
23	*C. leucodon*	Ctenomyidae (O)	4	71	*Octodontomys gliroides*	Octodontidae (O)	4
24	*C. magellanicus*	Ctenomyidae (O)	3	72	*Octomys mimax*	Octodontidae (O)	4
25	*C. peruanus*	Ctenomyidae (O)	2	73	*Olallamys albicauda*	Echimyidae (O)	2
26	*C. porteousi*	Ctenomyidae (O)	4	74	*Pattonomys occasius*	Echimyidae (O)	1
27	*C. pulcer*	Ctenomyidae (O)	1	75	*Phyllomys blainvillii*	Echimyidae (O)	1
28	*C. talarum*	Ctenomyidae (O)	4	76	*P. thomasi*	Echimyidae (O)	3
29	*C. torquatus*	Ctenomyidae (O)	2	77	*Plagiodontia aedium*	Echimyidae (O)	2
30	*C. yolandae*	Ctenomyidae (O)	2	78	*Proechimys brevicauda*	Echimyidae (O)	2
31	*Dactylomys boliviensis*	Echimyidae (O)	2	79	*P. canicollis*	Echimyidae (O)	4
32	*D. dactylinus*	Echimyidae (O)	2	80	*P. chrysaeolus*	Echimyidae (O)	3
33	*Dasyprocta azarae*	Dasyproctidae (Ca)	4	81	*P. guyannensis*	Echimyidae (O)	3
34	*D. fuliginosa*	Dasyproctidae (Ca)	4	82	*P. oconnelli*	Echimyidae (O)	3
35	*D. punctata*	Dasyproctidae (Ca)	5	83	*Spalacopus cyanus*	Octodontidae (O)	3
36	*Dinomys branickii*	Dinomyidae (Ch)	3	84	*Thrichomys*	Echimyidae (O)	3
37	*Diplomys labilis*	Echimyidae (O)	3	85	*T. inermis*	Echimyidae (O)	1
38	*Dolichotis patagonum*	Caviidae (Ca)	5	86	*T. laurentius*	Echimyidae (O)	2
39	*D. salinicola*	Caviidae (Ca)	3	87	*Toromys grandis*	Echimyidae (O)	1
40	*Echimys chrysurus*	Echimyidae (O)	2	88	*T. rhipidurus*	Echimyidae (O)	2
41	*Erethizon dorsatum*	Erethizontidae	3	89	*Trinomys albispinus*	Echimyidae (O)	4
42	*Euryzygomatomys spinosus*	Echimyidae (O)	1	90	*T. iheringi*	Echimyidae (O)	5
43	*Galea comes*	Caviidae (Ca)	4	91	*T. nigrispinus*	Echimyidae (O)	1
44	*G. leucoblephara*	Caviidae (Ca)	2	92	*T. paratus*	Echimyidae (O)	2
45	*G. spixii*	Caviidae (Ca)	3	93	*T. yonenagae*	Echimyidae (O)	1
46	*Geocapromys brownii*	Echimyidae (O)	1	94	*Tympanoctomys aureus*	Octodontidae (O)	4
47	*Hoplomys gymnurus*	Echimyidae (O)	3	95	*T. loschalchalerosorum*	Octodontidae (O)	1
48	*Hydrochoerus hydrochaeris*	Caviidae (Ca)	3	96	*T. barrerae*	Octodontidae (O)	3